51st AIAA Aerospace Sciences Meeting including the New Horizons Forum and Aerospace Exposition
07 - 10 January 2013, Grapevine (Dallas/Ft. Worth Region), Texas

AIAA 2013-0801

Simulated Rotor Wake Interactions Resulting from Civil Tiltrotor Aircraft Operations Near Vertiport Terminals

Larry A. Young[1]
Gloria K. Yamauchi[2]
NASA Ames Research Center, Moffett Field, CA, 94035

Ganesh Rajagopalan[3]
Iowa State University, Ames, IA 50011

A mid-fidelity computational fluid dynamics tool called RotCFD – specifically developed to aid in rotorcraft conceptual design efforts – has been applied to the study of rotor wake interactions of civil tiltrotor aircraft in the immediate vicinity of vertiport/airport ground infrastructure. This issue has grown in importance as previous NASA studies have suggested that civil tiltrotor aircraft can potentially have a significant impact on commercial transport aviation. Current NASA reference designs for such civil tiltrotor aircraft are focused on a size category of 90-120 passengers. Notional concepts of operations include simultaneous non-interfering flight into and out of congested airports having vertiports, that is, prepared VTOL takeoff and landing zones, or underutilized short runways for STOL operation. Such large gross-weight vehicles will be generating very high induced velocities. Inevitably, the interaction of the rotor wake with ground infrastructure such as terminal buildings and jetways must be considered both from an operational as well as design perspective.

Nomenclature

C_p	=	pressure coefficient
C_P	=	rotor power coefficient
C_T	=	rotor thrust coefficient
FM	=	rotor hover figure-of-merit
FM_∞	=	rotor hover figure-of-merit out-of-ground-effect
h	=	rotor height above ground
R	=	rotor radius
v_w	=	wind speed
x	=	horizontal distance from vertical wall or plane or building to rotor center
$\Delta\psi$	=	wind direction with respect to aircraft; 0 deg towards the aircraft nose

I. Introduction

IT has long been envisioned that rotorcraft in general, and tiltrotor aircraft in particular, might one day play a significant role in commercial transport aviation. Several NASA-sponsored studies over the past two decades have reinforced this vision of commercial transport rotorcraft. Recent studies, Refs. 1-3, have focused on tiltrotor aircraft in the size category of 90-120 passengers. Such studies have shown that large civil tiltrotors can have a significant influence on reducing National Airspace System (NAS) delays and increasing throughput. To accomplish such gains requires development of vertiports (prepared VTOL takeoff and landing zones) and using

[1] Aerospace Engineer, Aeromechanics Branch, Flight Vehicle Research and Technology Division, Mail Stop 243-
[2] Aerospace Engineer, Aeromechanics Branch, Flight Vehicle Research and Technology Division, Mail Stop 243-12.
[3] Professor, Department of Aerospace Engineering.

short, underutilized runways at congested airports. Figure 1 is a simple illustration of a notional airport layout in which there is both a vertiport terminal and short runway for tiltrotor operations. A major consideration in the development of vertiports co-located at airports is the magnitude of rotor/wake interactions (i.e. in-ground-effect groundwash) from such large vehicles in close proximity to ground infrastructure.

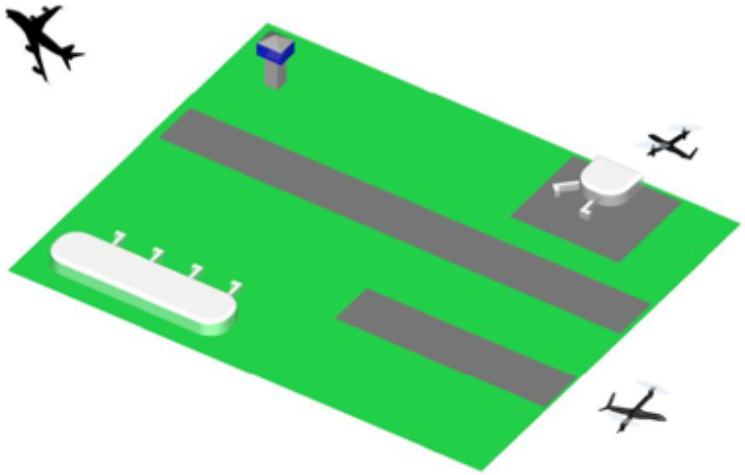

Figure 1. Vertiport tiltrotor operations at airport (VTOL and STOL).

In order to assess the compatibility of the NASA civil tiltrotor (CTR) reference designs with the anticipated Concept of Operations (CONOPS) of such aircraft operating into and out of major congested airports (circa ~2025) computational fluid dynamics (CFD) tools are required to predict rotor/wake interactions, particularly rotor groundwash, in the immediate vertiport/terminal area. The CFD tool of choice for this study is RotCFD (Ref. 4). RotCFD is a mid-fidelity tool aimed at conceptual design. The technical approach for this study is to begin with simple rotor in-ground-effect (IGE) predictions, then proceed to dual side-by-side rotor IGE predictions, followed by a complete Large Civil Tiltrotor (LCTR2) aircraft (Ref. 5) IGE predictions. Walls, planes and simple geometric shapes representing buildings are then introduced, concluding with a LCTR2 aircraft operating near a more realistic modeling of a vertiport terminal facility. Figure 2 and 3 illustrate the ultimate problem to be studied: strong rotor wakes from hovering civil tiltrotor aircraft impinging upon and blowing along the ground and up against ground infrastructure. These large rotor wake downwash and groundwash velocities, in turn, result in substantial pressure loading on building structures.

RotCFD will first be validated for rotor wake interaction problems. Comparisons will be made with full-scale tiltrotor outwash data (Ref. 6). In addition, single- and dual-rotor IGE predictions will be compared to analytical results from Refs. 7-9.

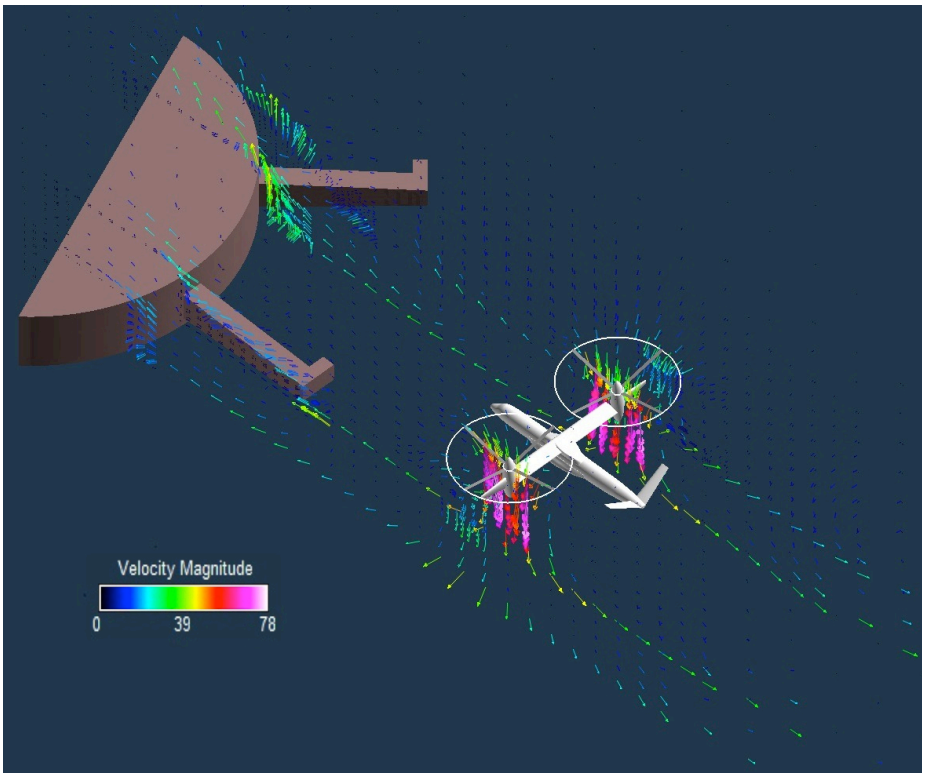

Figure 2. Rotor wake interaction of a civil tiltrotor in the vicinity of a vertiport (velocity field shown).

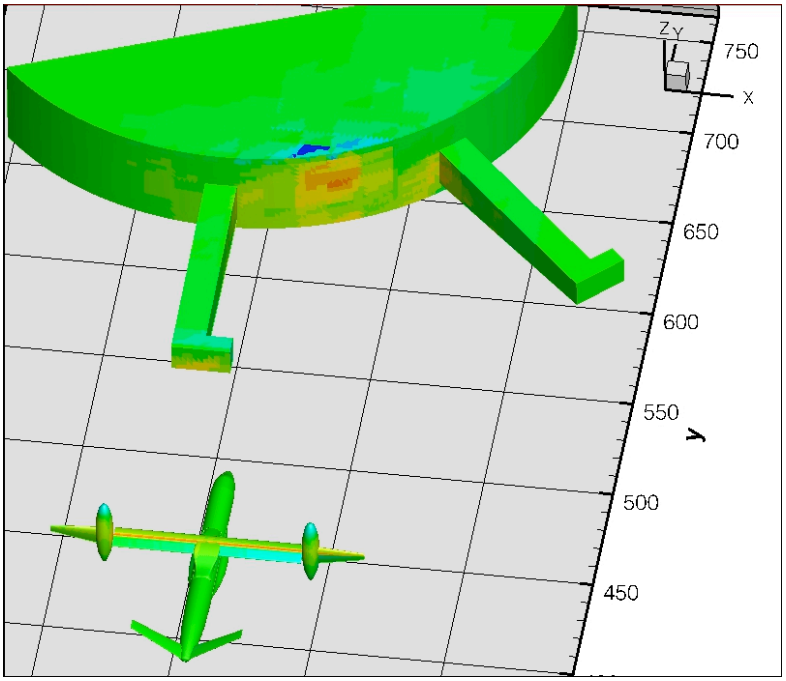

Figure 3. Rotor wake interaction of a civil tiltrotor in the vicinity of a vertiport (surface pressures shown on aircraft and building).

II. Description of Analysis Approach

A. RotCFD Computational Fluid Dynamics Tool

RotCFD attempts to bridge the two worlds of design and Computational Fluid Dynamics (CFD) with the help of an Integrated Design Environment (IDE) specific to rotorcraft. RotCFD emphasizes user-friendliness and efficiency that streamline the design process from geometry to CFD solution. The key components of RotCFD are a geometry module, a semi-automated grid generation module, a flow-solver module, a rotor module, a flow visualization module, and an analysis module, all integrated in one environment. The concept of rotor blades represented by momentum sources forms the basis of this aerodynamic simulation tool for rotorcraft. The rotor momentum sources are primarily a function of the local velocity of the flow and the two-dimensional airfoil characteristics of the rotor blades. The Navier-Stokes equations and the blade element theory are coupled implicitly to yield a self-contained method for generating performance, as well as the near and far wake including all the aerodynamic interference inherent in a situation.

During initial design studies, parametric variation of vehicle geometry is routine. A simple geometry tool (modest CAD functionality) is offered to simplify geometry manipulation. The current version of RotCFD can read the body geometry in STL or Plot3D format. Also, some simple shapes (bodies of revolution) can be generated from within RotCFD. In addition to general transformations such as translation, rotation and scaling, parametric variation of the geometry is available to assist with the design. Graphical visualization is used to make the geometry manipulation user-friendly: the user is able to see a preview of the geometry change before committing the change.

The RotCFD Cartesian unstructured (hanging node) grid is economical to generate and can be completely automated. The cells that intersect the body, and all the cells that immediately surround the intersected cells are replaced by tetrahedra. The simple shape of the tetrahedron allows the grid to be morphed slightly in order to conform to the body. Thus the body conforming grid generator modifies a Cartesian grid (Cartesian here meaning all faces are aligned with the Cartesian planes) such that the grid will approximately conform to the surface of the body. The grid is approximate since the algorithm only considers the intersections between the surface geometry and the edges of the original grid. New surface faces are generated based on those edge-surface intersections instead of using the original polygons from the surface geometry. This approximate approach avoids the technical difficulties associated with maintaining the surface geometry exactly as it intersects the grid, and allows the development of a simpler and more robust algorithm with a much shorter development time. The approach also has the advantage that clean geometries are not required, only that they be closed surfaces.

The flow field of a rotor is complex; even an isolated rotor is dominated by the mutual, aerodynamic interference effects of the blades. Therefore, all simulation techniques, to be successful, must consider interference effects. The SIMPLER/SIMPLE (Ref. 10) line of pressure-based algorithms to solve the Navier-Stokes equations is suitable for low speed flows and currently SIMPLE is used for solving the flow field in RotCFD. Additional details describing RotCFD are summarized in Ref. 4.

During the course of this work two different beta versions of RotCFD were employed: version 9.11 and 9.13. Version 9.11 provided laminar flow only solutions and version 9.13 provided both laminar and turbulent solutions. The turbulence model in RotCFD 9.13 employed in this study was the “realizable k-e” model; for more details refer to Ref. 11. As appropriate, the particular RotCFD version number will be cited wherever results are presented.

B. The LCTR2 Reference Design Vehicle

The baseline vehicle design used in this study is a NASA reference design described in Ref. 5. The LCTR2 is a 90-passenger vehicle and has been used in many past studies. Alternate large civil tiltrotor vehicle conceptual designs are available, e.g. the vehicle designs detailed in Refs. 1-3, but the LCTR2 reference design is perhaps the most well known. The RotCFD models are based on CAD geometry files that have been recently used to fabricate

small-scale wind tunnel models of the LCTR2 vehicle. The LCTR2 reference design is currently used within the NASA Rotary-Wing project to aid in guiding its technology portfolio.

An initial assessment of RotCFD's rotor performance predictive capability is shown Fig. 4. Figure 4 compares LCTR figure of merit (FM) out-of-ground-effect (OGE) calculated by RotCFD and the comprehensive rotorcraft analysis CAMRAD II. CAMRAD II is a lifting-line/lifting-surface code using a free-wake model for the rotor wake and uses C81 airfoil tables to calculate the sectional blade aerodynamic loads. The RotCFD results are generally comparable to the CAMRAD II results (taken from Ref. 5) with the exception that RotCFD seems to predict rotor stall at a lower thrust than CAMRAD II. Extensive rotor and tiltrotor experimental data correlation (e.g. Ref. 12) with CAMRAD II predictions necessitated the incorporation of stall delay models in order to correctly predict the high-thrust rotor characteristics of tiltrotors. Figure 4 suggests that future versions of RotCFD should also incorporate stall delay models to improve overall predictive capability.

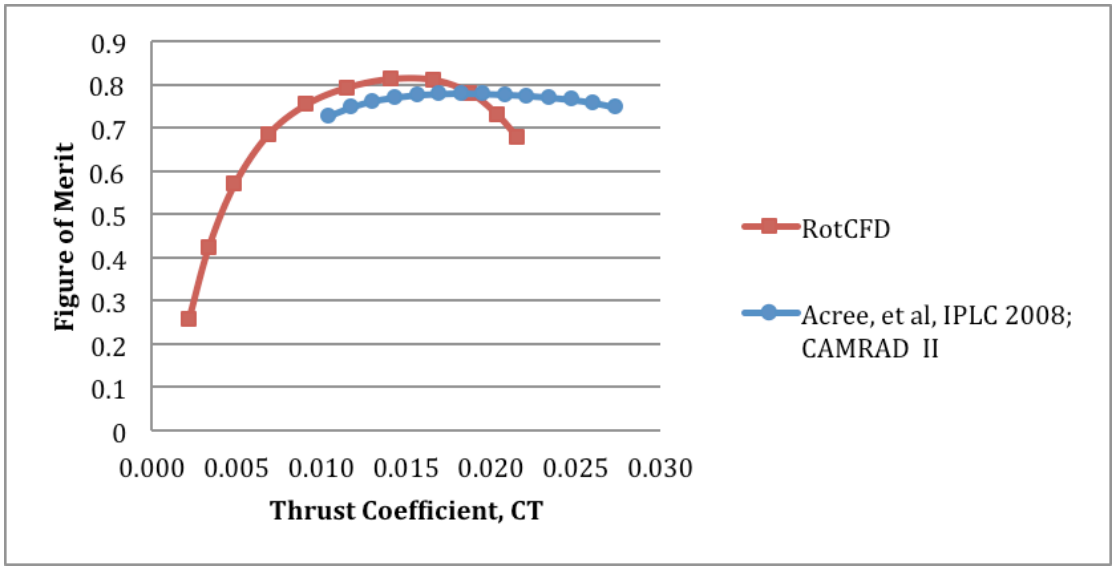

Figure 4. Comparison of LCTR2 reference design isolated rotor (OGE) hover performance predictions

C. Notional Terminal/Vertiport Layouts

The principal guide for vertiport design used in this study is Ref. 13. This FAA Advisory Circular, initially released in the mid-1990s, has subsequently been canceled, but still represents the best source of vertiport design guidance available. The notional vertiport layout illustrated in Figs. 2-3 is somewhat inspired by specific terminals at Newark Liberty International airport. However, one of the key challenges of this study is to derive general results for rotor/wake interactions for CTR operating near vertiports and other airport ground infrastructure that are not unduly biased by the models used for such ground infrastructure. Before presenting the vertiport modeling results a number of simpler modeling cases will be examined, including the influence of ground- and wall-planes on tiltrotor performance.

III. Validation with Full-Scale Outwash Measurements

An unique set of rotor outwash measurements was acquired in 1998 to support FAA research in vertiport/heliport operations. The outwash profile of a V-22 aircraft with wheels on the ground and with the aircraft at several heights above ground are documented in Appendix A of Ref. 6. With wheels on the ground, profiles were measured in two directions: along the aircraft center line (azimuth = 0), and along an axis intersecting the two rotors on the port/left side of the aircraft (azimuth = 270 deg). Mean and peak velocities were measured in 1-ft increments above the ground between 1ft and 7 ft for four different aircraft thrusts.

A RotCFD simulation was performed using two isolated V-22 rotors positioned at the same height as the V-22 wheels-on-ground experiment of Ref. 6. Figure 5a shows the two grid refinement boundaries within the computational domain. A cross-section of the grid system at x=0 is shown in Figure 5b. As shown in Figs. 5 and 6, the domain boundaries were approximately Y = ±8D, X = ±6D, and Z = -0.56D to approximately 4D. The simulation was run for 21 simulated seconds. The solution at each of the last 5 seconds was saved and an average solution was computed from the five saved solutions. RotCFD does not currently have the capability to trim the rotors to a specified thrust, so a collective pitch was selected to provide a thrust level within the range (9950-33810 lb) measured by the experiment. For the simulation presented here, a collective pitch of 8.5 deg provided 23326 lb of thrust. Matching the measured thrust precisely was not critical as the correlation between experiment and simulation is presented using nondimenional parameters. The rotor diameter, D = 2R =38 ft, was used to nondimensionalize the distance from the aircraft centerline. The hover induced velocity, V_h = (aircraft thrust/$(4*\rho*\pi*R^2)$)$^{1/2}$, was used to nondimensionalize the maximum mean velocity, $Vmax_{avg}$, from each velocity profile.

Figure 7 provides a sample flow field result from the validation test case. Figs. 8a and 8b present $Vmax_{avg}/ V_h$ as function of the nondimensional distance in front of the aircraft and to the port/left side of the aircraft, respectively. As expected, the computed maximum mean velocity beneath or close to the rotors is not captured well since the fuselage, hubs, and nacelles were not modeled. However, at a distance of 2D from the the aircraft centerline, the computed $Vmax_{avg}/ V_h$ tracks quite well with the measurements, except near Y=4D (Fig. 8b)). Further grid refinements and incorporation of a representative fuselage, hub, and nacelle may improve the comparison closer to the rotor. Away from the rotor, however, the computed outwash of two isolated rotors provides a good approximation to the measurements.

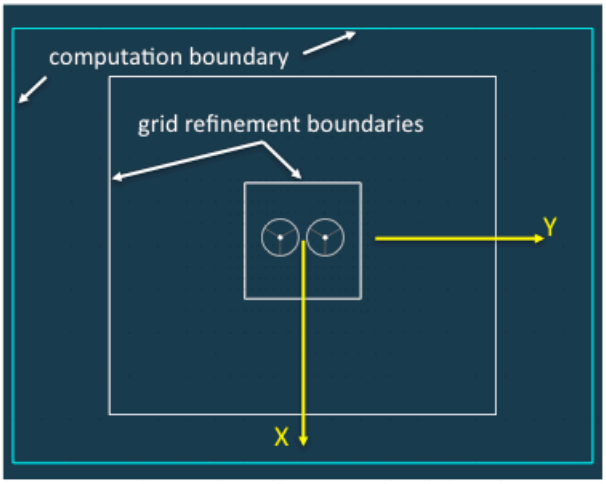

a) Top view of computational domain

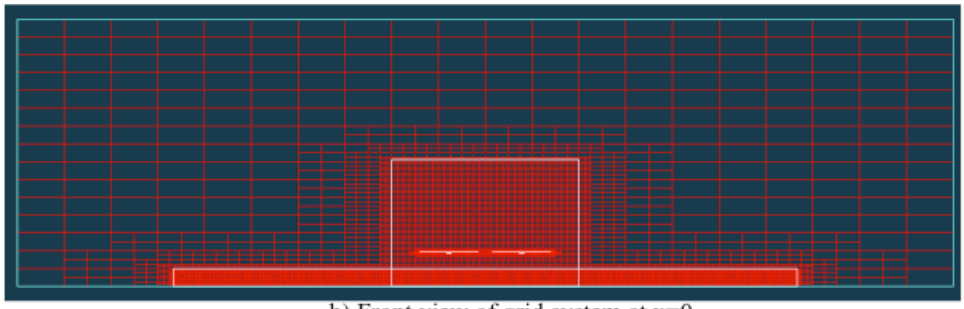

b) Front view of grid system at x=0

Figure 5. RotCFD computational domain.

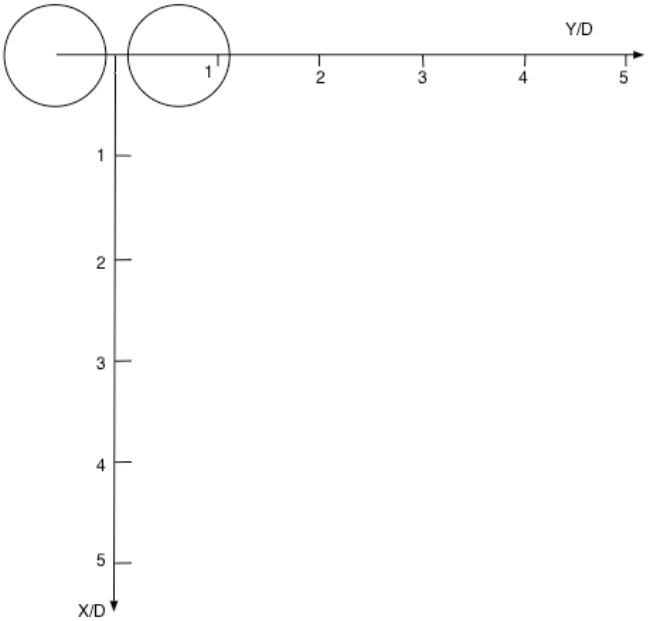

Figure 6. RotCFD nondimensional coordinate system.

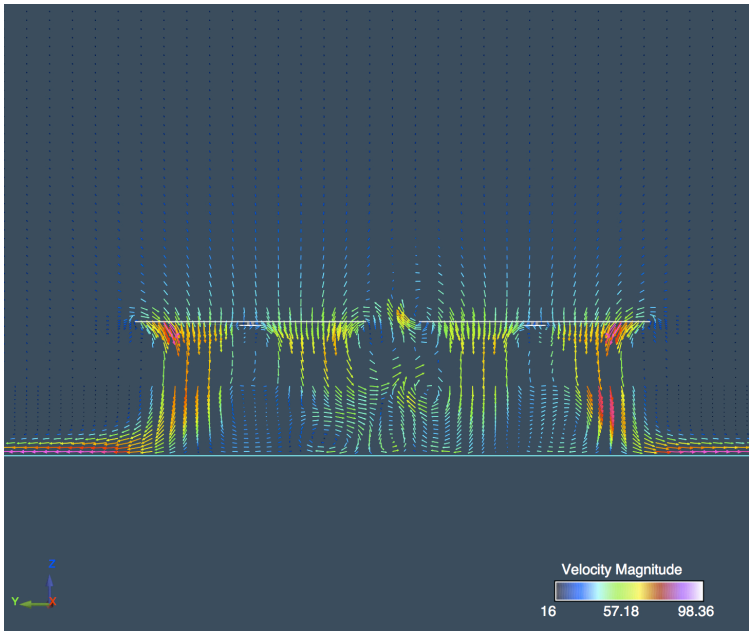

Figure 7. RotCFD flow field prediction of the dual rotor configuration used in the groundwash profile distribution validation

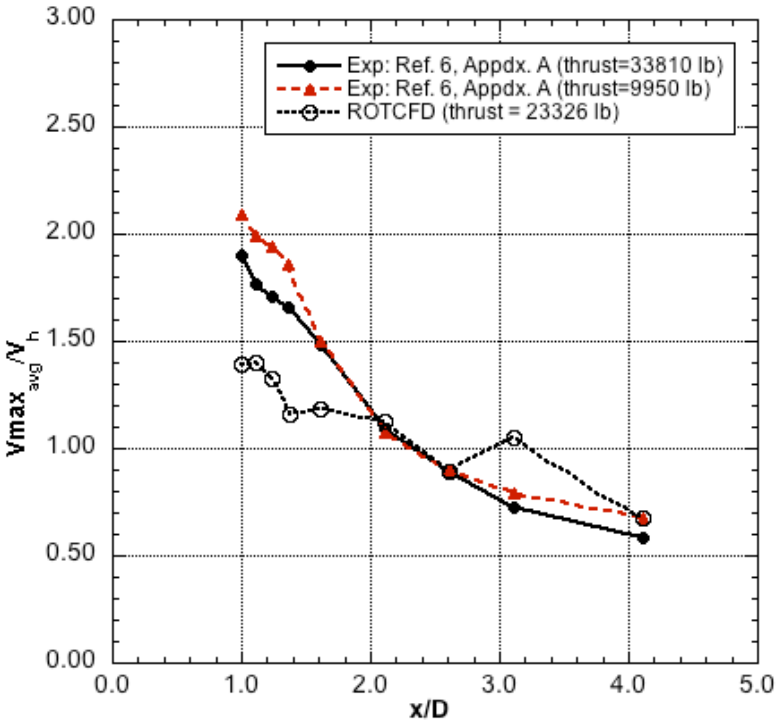

a) Maximum average velocity in front of aircraft along aircraft centerline (azimuth = 0 deg)

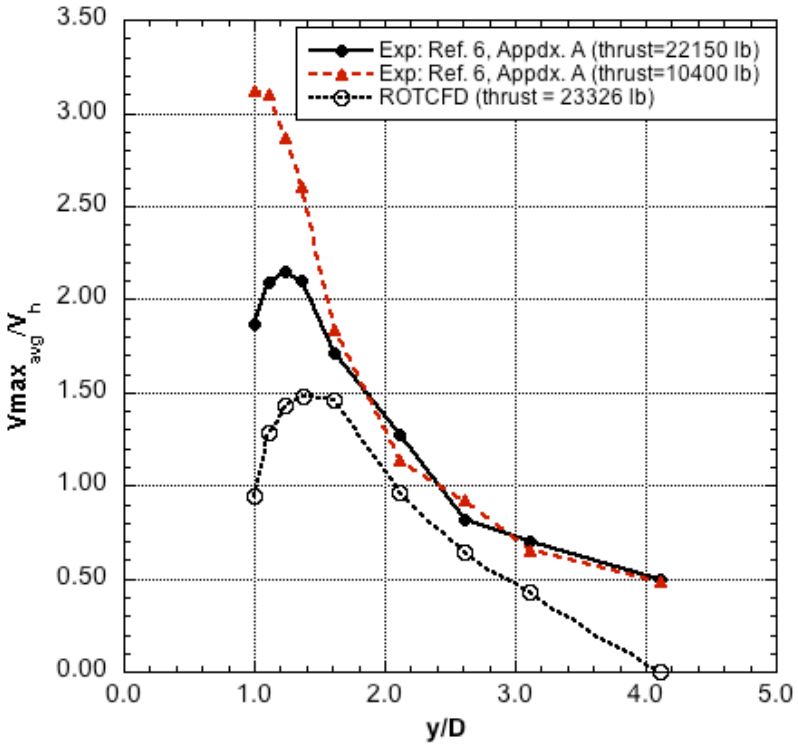

b) Maximum average velocity along axis passing through rotors (azimuth = 270 deg)

Figure 8. Comparison of measured (Ref. 6) and computed outwash velocities

IV. LCTR2 Simulation Results

The issue of rotor wake interactions was examined by incrementally modeling the problem from simple to more complex geometries. Pursuing this methodical approach provided improved insights to the overall problem. Accordingly, RotCFD results will presented in the following order: a single isolated LCTR2 rotor in hover for both IGE and OGE; a single LCTR2 rotor in forward-flight IGE; dual LCTR2 rotors (with no wing or airframe) in hover IGE; a full LCTR2 vehicle in hover IGE; a LCTR2 vehicle in hover in close proximity to both ground- and wall-planes; a LCTR2 vehicle yawed with respect to a wall-plane; a LCTR2 vehicle at several locations in close proximity to a vertiport; and a LCTR2 vehicle in close proximity to airport surface infrastructure and a small general-aviation aircraft.

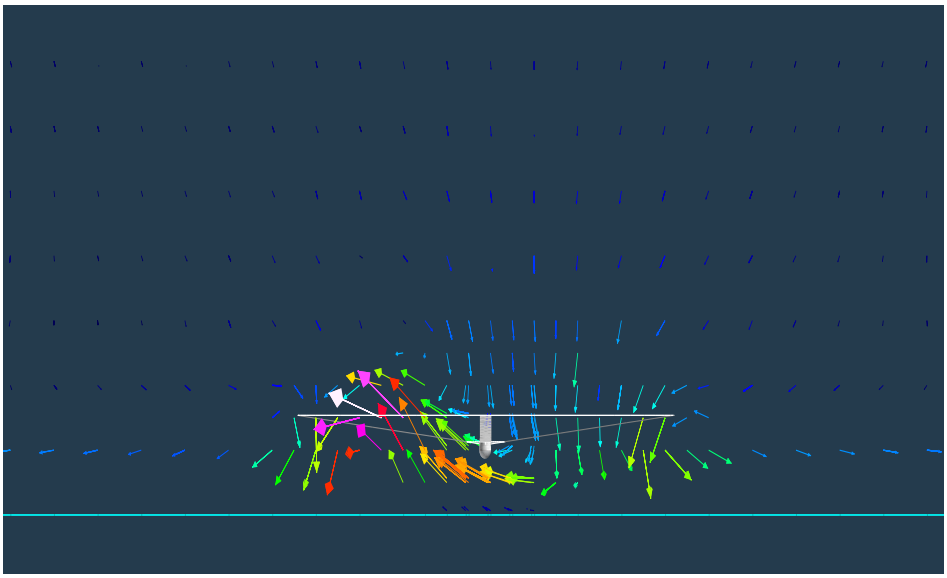

(a) h/R = 0.25

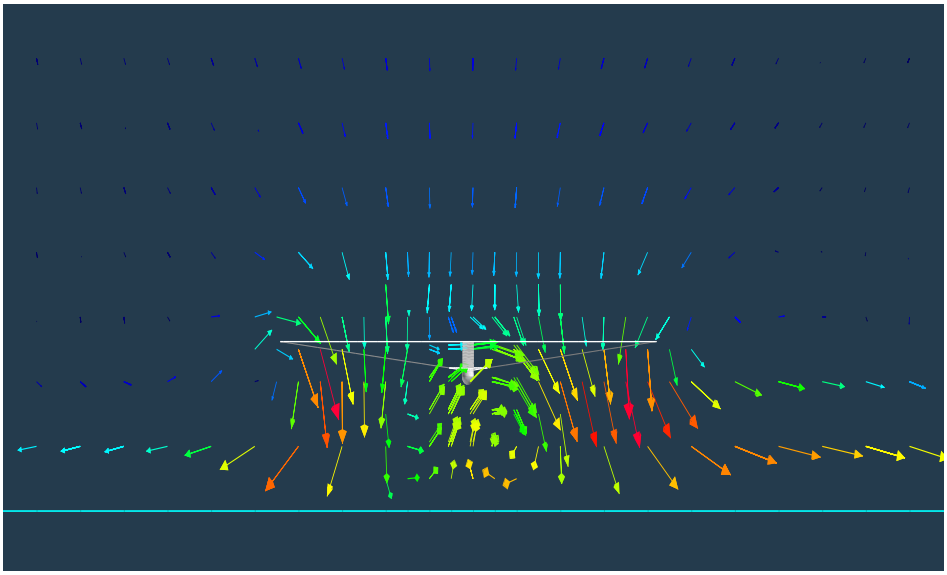

(b) h/R=0.5.

Figure 9. Single rotor above ground plane

A. LCTR2 Rotor/Vehicle Configuration Build-Up and Parametric Sweeps

Figure 9 presents the velocity flow field of a single LCTR rotor at several different heights above a ground-plane. The rotor collective pitch was set to 20 deg. The RotCFD results represent the unsteady Navier-Stokes solution at the prescribed maximum time duration for the solution. This maximum time duration and the commensurate time steps were iteratively determined during early test runs to insure that the rotor performance coefficients had asymptotically approached nominal value.

As shown in Fig. 9, there is considerable asymmetry (though intuitively symmetry is expected) observed in the hover IGE rotor flow, particularly at the lower value of h/R (Fig. 9a). At the larger h/R value (Fig. 9b), the rotor wake approaches a symmetrical flow.

Figure 10 presents the IGE rotor performance results for the single LCTR2 rotor. RotCFD predictions were made for collective pitches of 10 and 20 deg. Also provided in Fig. 10 are two other predicted IGE performance curves based on the work of Cheeseman and Bennett (Ref. 14) and Hayden (Ref. 15). In general, the RotCFD prediction trend is in agreement with the two classic analyses except, not unexpectedly, for very low h/R values. Less clear is why the RotCFD curves are not smooth for h/R>1. Though a nontrivial effort was expended trying to address this issue, this behavior is possibly a consequence of inadequate RotCFD grid refinement levels and inadequate refinement box definition.

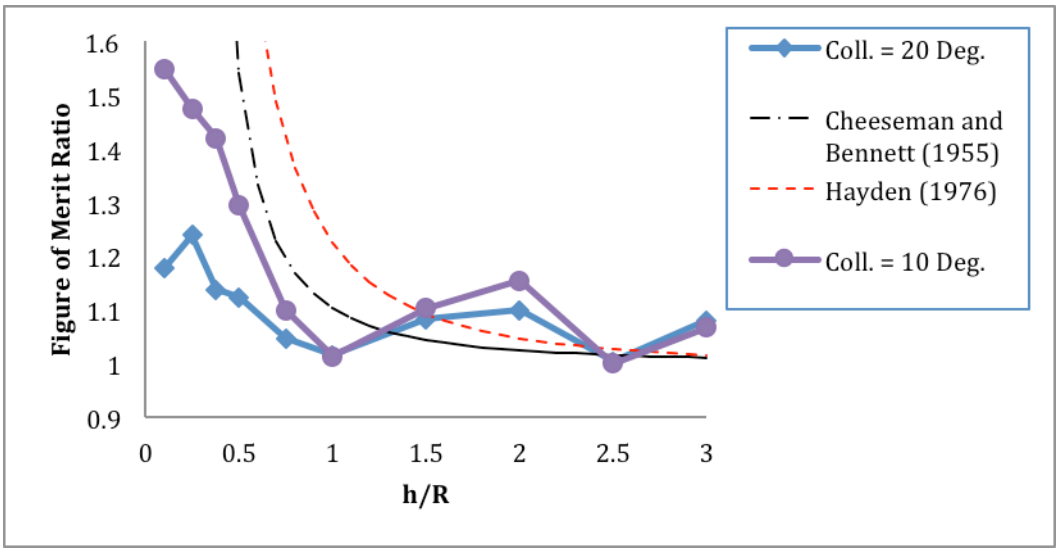

Figure 10. Hover performance of a single LCTR2 rotor in-ground-effect

Figure 11 illustrates the behavior of a single LCTR2 rotor IGE with freestream velocity of V=13 fps or 4 m/s, an effective advance ratio of μ=0.02. The "horseshoe" ground vortex at the forward edge of the rotor disk (left hand region of Fig. 11a, near the ground-plane) can be clearly seen in the velocity vectors mapping the rotor flow field and the velocity isosurface in Figs.11a and 11b, respectively. The single LCTR2 rotor is at ten deg. of collective; no cyclic trimming of the rotor has been performed. This result is representative of not only very low-speed forward-flight but also rotor flow behavior in cross-winds. Several cases were studied for the single rotors in low-speed flight/cross-winds at different rotor collectives, and h/R ratios (in- and out-of-ground-effect).

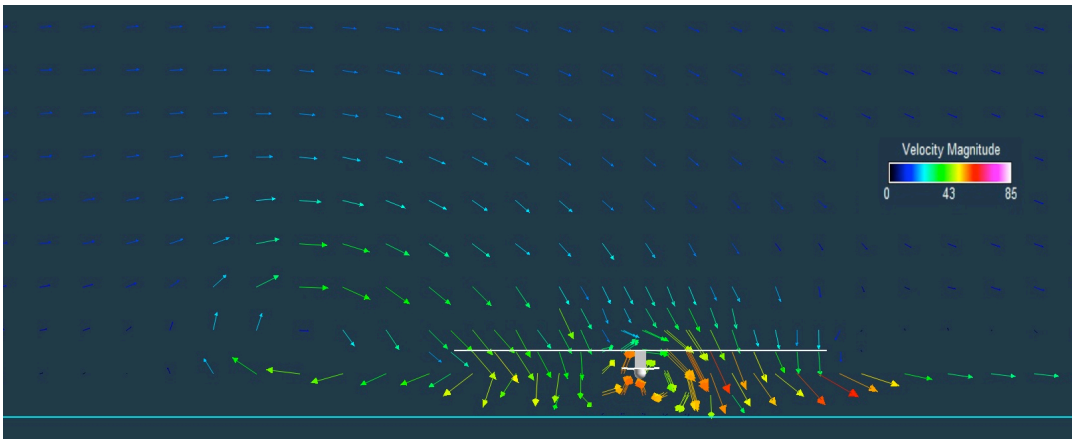

(a) velocity vector field

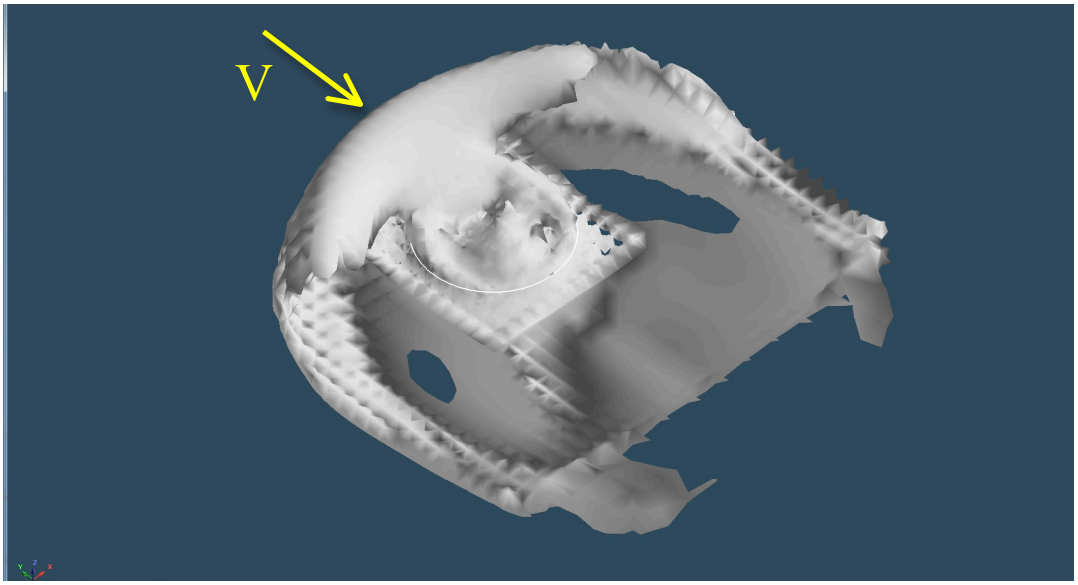

(b) velocity magnitude isosurface

Figure 11. Single LCTR rotor IGE, h/R= 0.25, freestream velocity V = 4m/s.

Figure 12 illustrates rotor performance characteristics of a single LCTR2 rotor IGE in edgewise flight at a nominal thrust coefficient of C_T=0.012 (using the same nominal conditions of Fig. 11). RotCFD does not currently have a rotor thrust trim option. Consequently, rotor performance estimates were made at various collective settings; the power coefficients for the target rotor thrust coefficients were extracted using linear interpolation. Cyclic pitch at the blade root was not applied to trim the rotor moments. The general rotor power coefficient trends are consistent with the original observations of Refs. 14 and 15. The influence of the ground on the rotor power for low advance ratios is evident; as the advance ratio increases the influence of the ground effect quickly diminishes as the rotor wake is blown aft of the rotor rather than impinging on the ground.

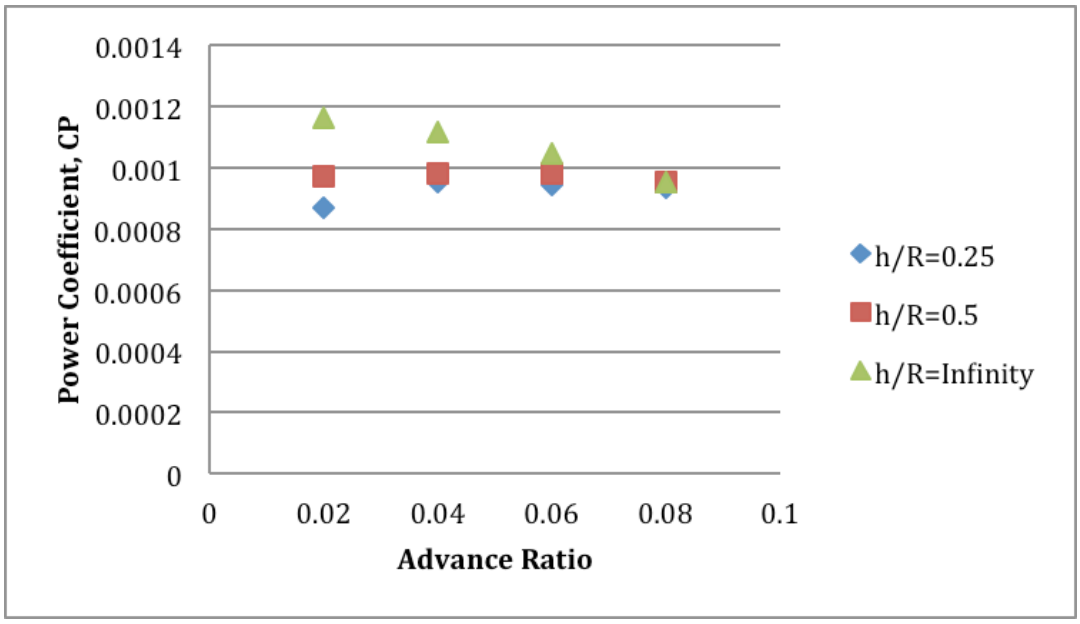

Figure 12. Effect of forward speed on the power of a single LCTR2 rotor in-ground-effect at a fixed C_T=0.012.

Figure 13 shows a comparison of rotor thrust predicted using the classic rotor performance theory of Ref. 14 and RotCFD (at two values of h/R). The trend agreement is acceptable.

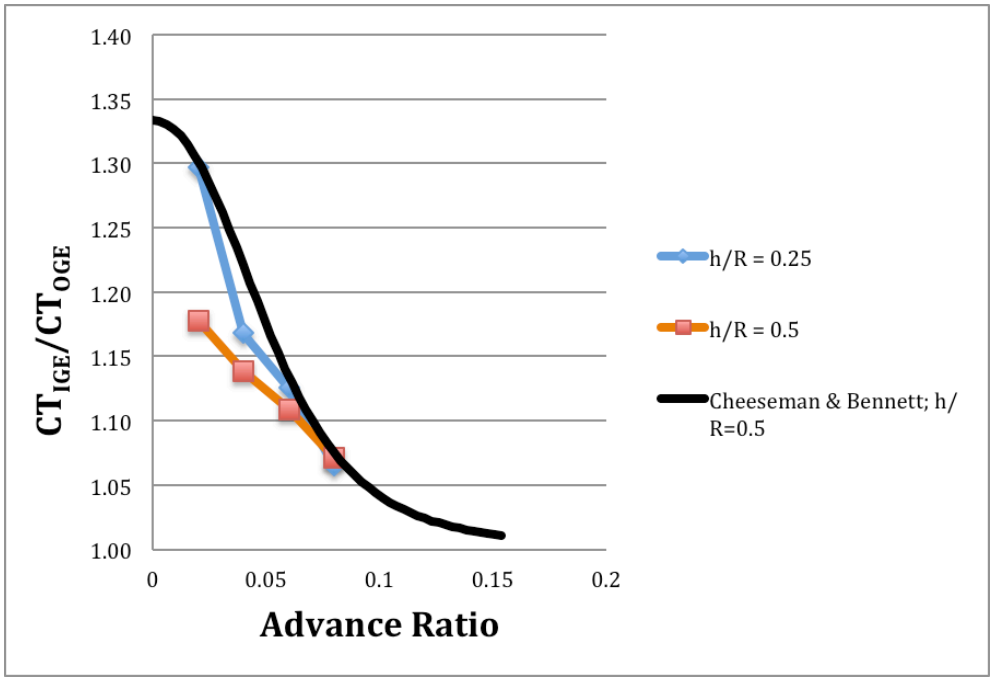

Figure 13. Effect of forward speed on the thrust of a single LCTR2 rotor in-ground-effect.

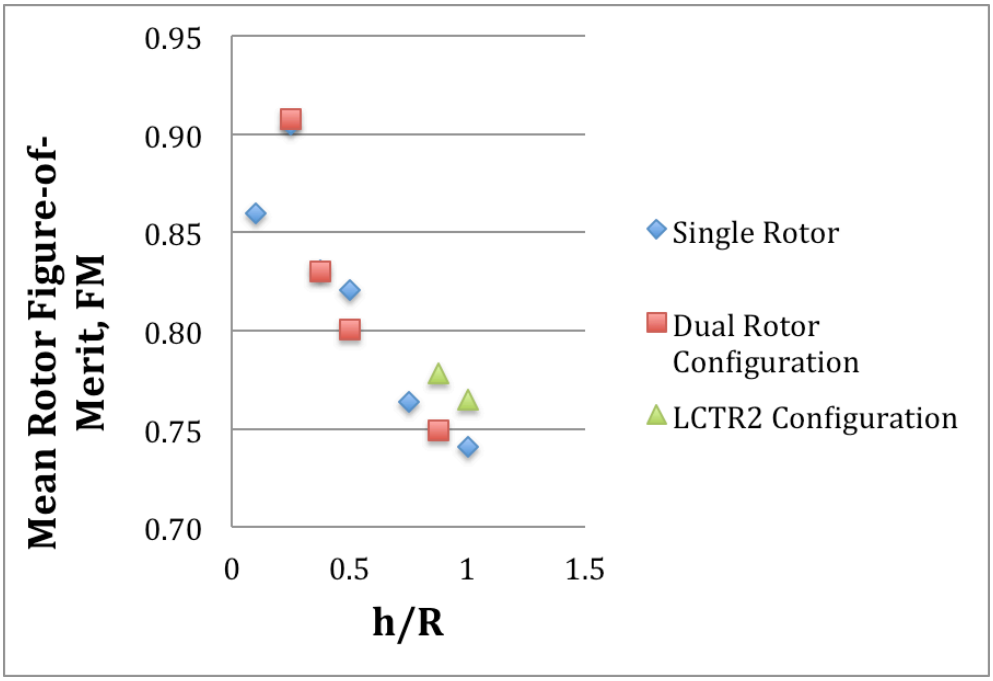

Figure 14. Comparison of hover IGE performance for a single rotor, dual rotors, and a LCTR2 vehicle.

Figure 14 compares the hover IGE rotor performance of a single LCTR2 rotor (presented in Fig. 10, for a collective pitch of 20 deg) with dual rotors and with the complete LCTR2 vehicle (rotor thrust only, airframe download not included). The FM results are only shown for h/R≤1 for all three configurations, as all three configurations suffer from spurious fluctuations observed in the RotCFD (Version 9.11) results for h/R>1. The spurious results likely stem from inadequate gridding refinement levels prescribed for the rotors and/or the lack of a stall-delay model in the analysis.

For h/R≤1, the RotCFD results in Fig. 14 suggest that the FM trends for the single and dual rotor configurations are approximately the same. The IGE FM for the LCTR2 vehicle shows a slight increase over the single and dual rotor configurations. The increase is caused by the download or "partial ground effect" of the vehicle fuselage and wing on the rotor performance. As the wing "body-fitting" refinement levels are set fairly low in the RotCFD model "partial ground effect" contribution is likely understated in the presented results.

Figure 15 is a comparison of the flow fields of the dual rotor configuration (no wing and no fuselage) versus the complete LCTR2 vehicle. The fountain effect over the wing between the two rotors is not properly captured in this initial set of test cases because the wing "body fitting' refinement levels were set fairly low.

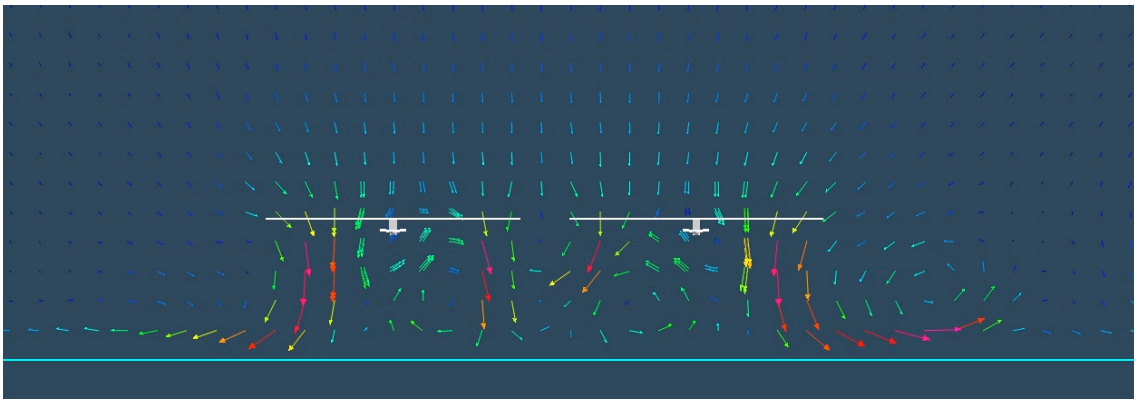

(a) LCTR2 Dual rotor configuration

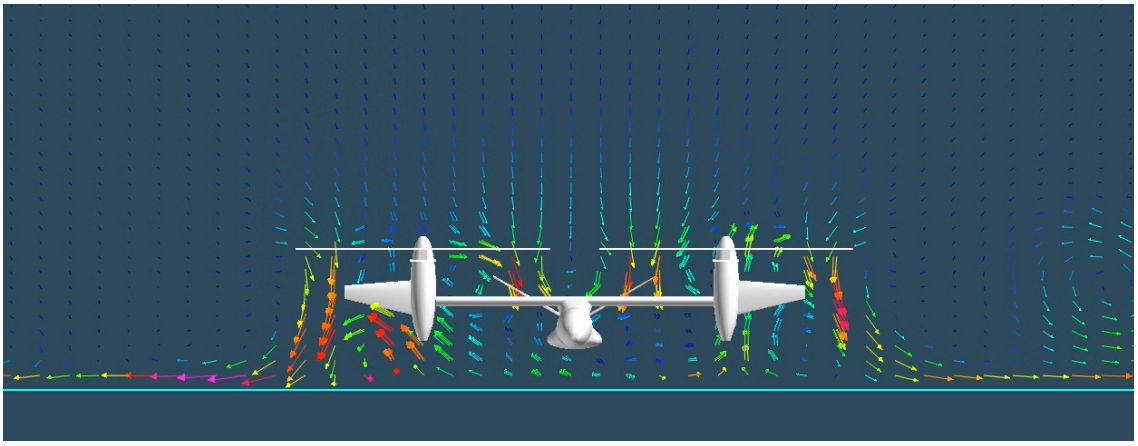

(b) LCTR2 vehicle

Figure 15. Front view of flow fields

B. Complete LCTR2 Vehicle Rotor/Wake Interactions with Ground and Side-Plane

As an incremental step towards modeling the wake interactions of the LCTR2 with vertiport terminal structures, a simpler case is considered: the rotor wake interactions with both a ground and a vertical side plane. The side plane represents a very large building. Figure 16 illustrates a series of flow field images for an x/R (nondimensional horizontal distance from the wall-plane) sweep.

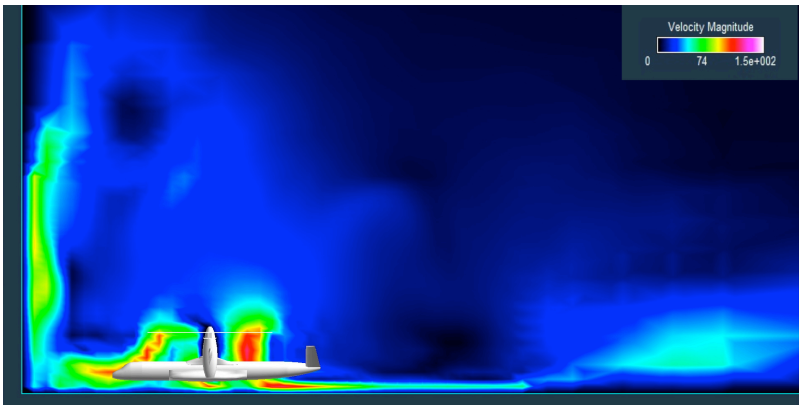

(a) x/R = 3

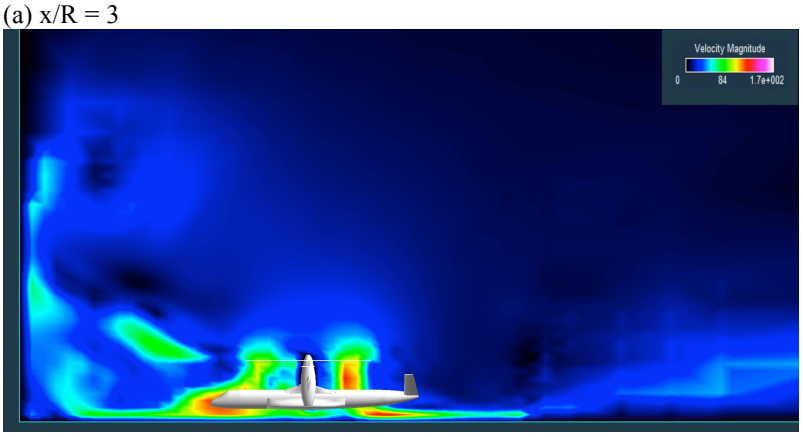

(b)x/R = 4.58

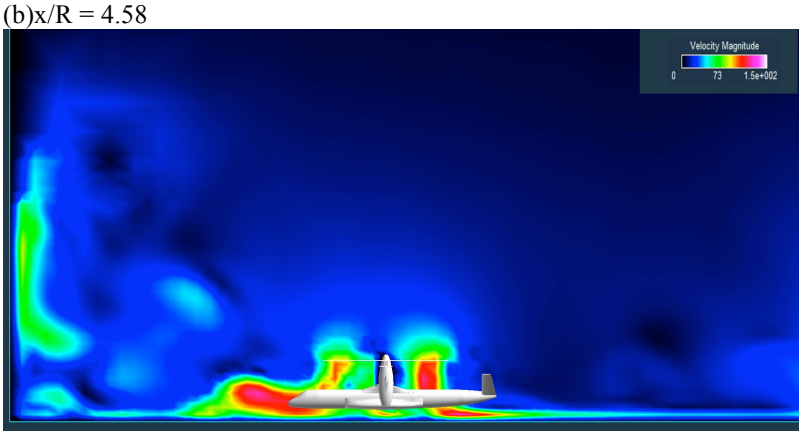

(c) x/R = 6

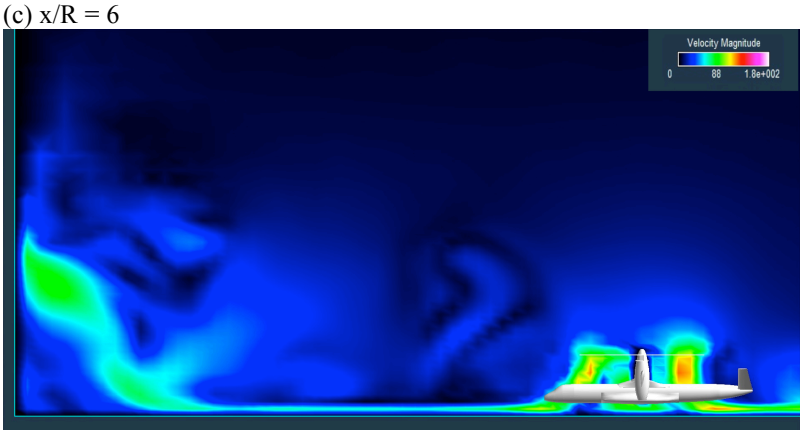

(d) x/R = 10

Figure 16. LCTR2 with ground plane and vertical side-plane (h/R=0.875)

RotCFD hover FM calculations for the x/R sweep (3≤x/R≤10) of Fig. 16 at h/R=0.875 is shown in Fig. 17. A small influence of x/R on the mean (the average of the two rotors) rotor FM is observed. An additional calculation for h/R = 1.5 is also included in Fig. 17.

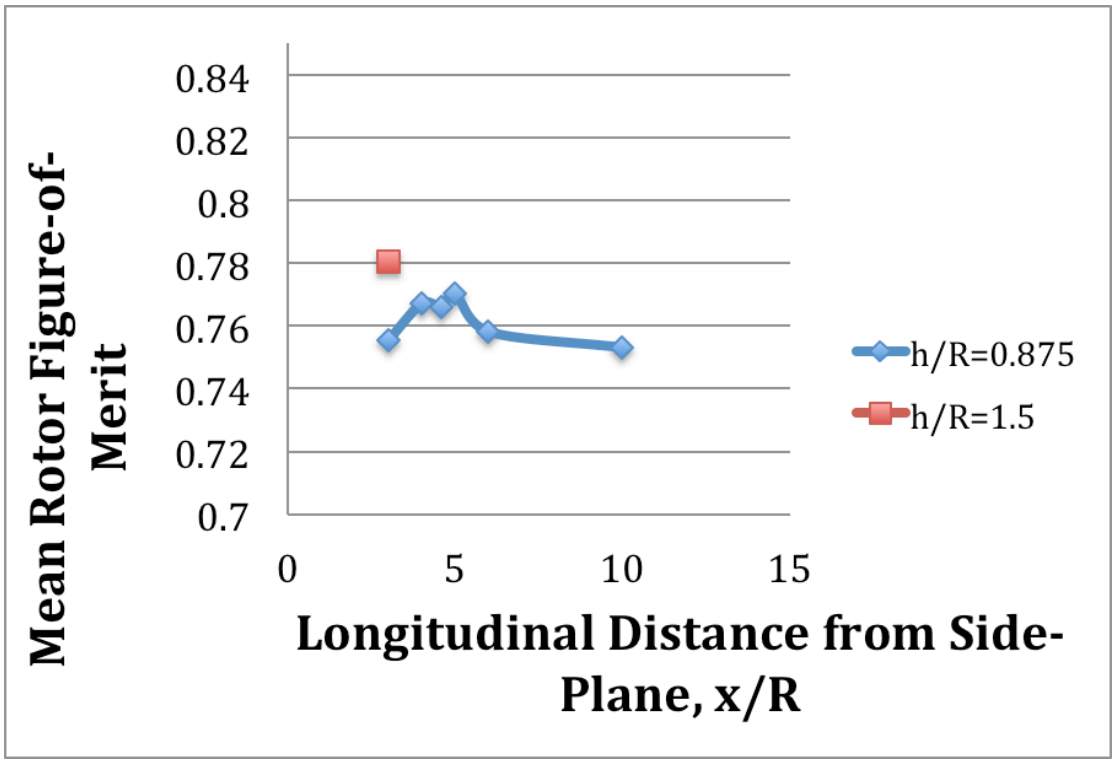

Figure 18 illustrates the wake interaction effects as the LCTR2 is yawed about the right-hand rotor axis so that the left-hand rotor is moved away from the vertical side-plane. Yawing the LCTR2 results in changes to the rotor wake flow recirculation next to, and above, the rotors. This, in turn, yields a small but significant influence on the vehicle nondimensional rolling moment (considering only the rotor contribution) as shown in Fig. 19.

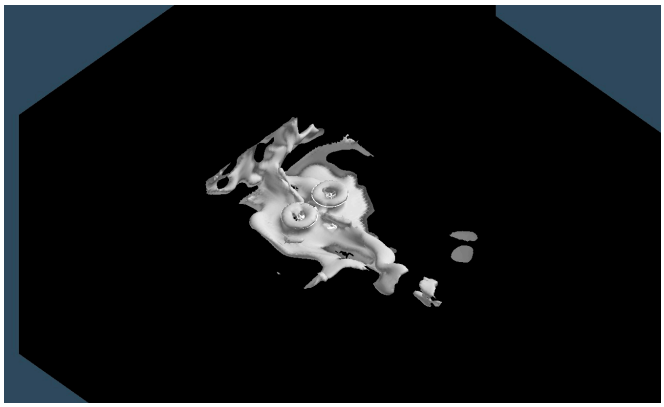

b) Yaw angle = 0 deg

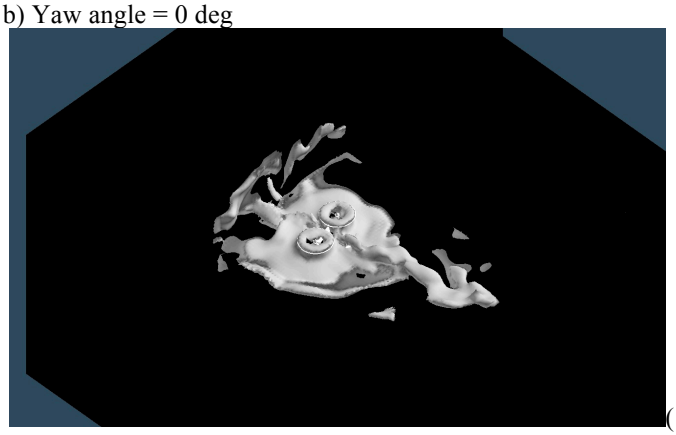

b) Yaw angle = 15 deg

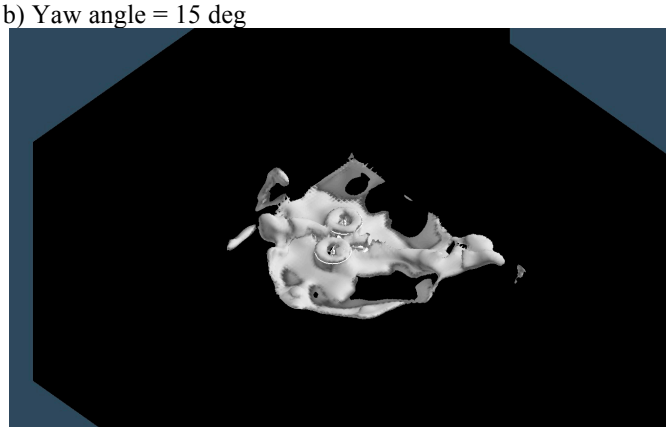

(c) Yaw angle = 30 deg

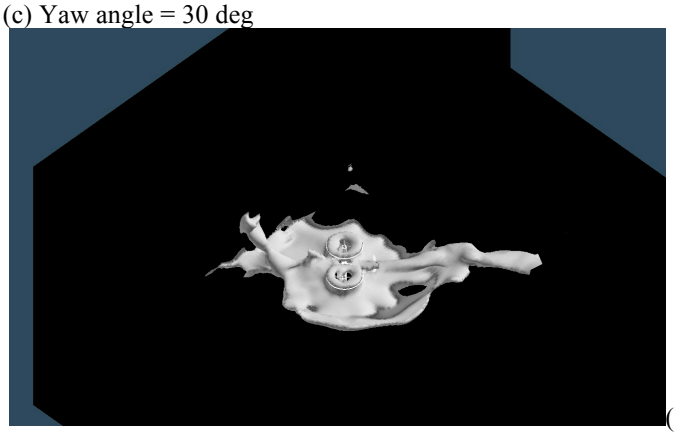

d) Yaw angle = 45 deg

Figure 18. LCTR2 with ground plane and vertical side-plane (h/R=0.875 and x/R=4)

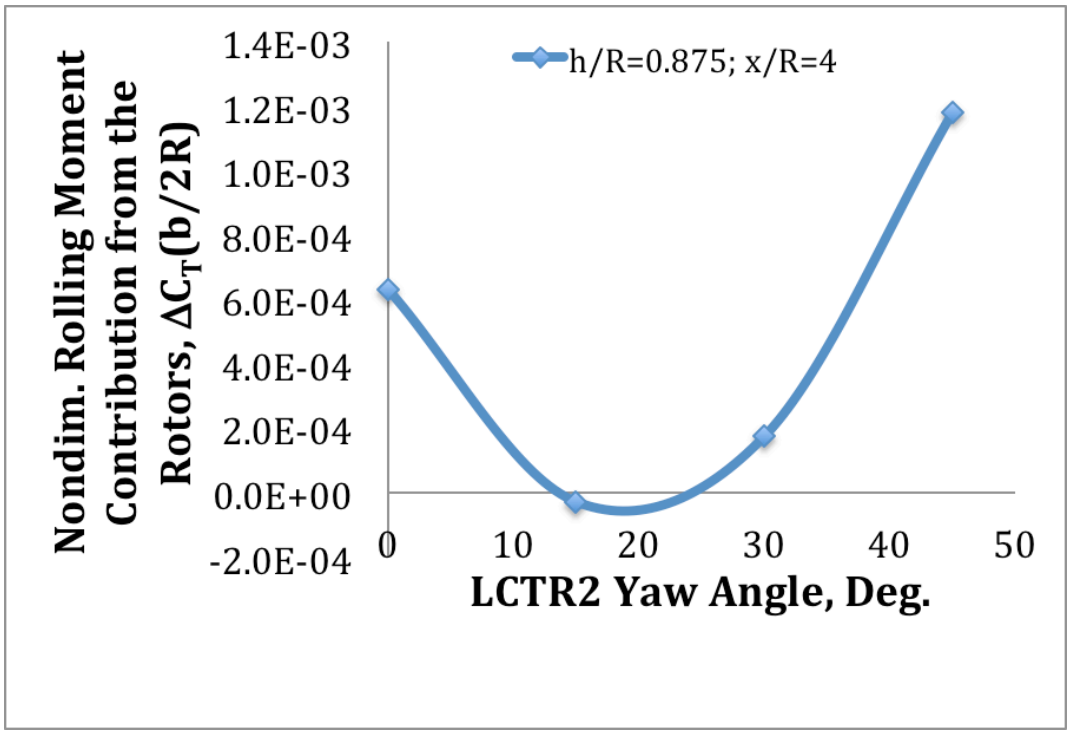

Figure 19. Nondimensional rolling moment contributions from the rotors for the LCTR2 in hover IGE in close proximity to a side-plane

C. Rotor Wake Interactions for Vertiport Configurations

Figures 20a-20c illustrate the LCTR2 aircraft near a notional vertiport building for increasing vehicle height. When the vehicle is in IGE, the rotor groundwash significantly interacts with the vertiport terminal building. A key consideration for future civil tiltrotor operation is the question of how far away from the vertiport terminal building does the aircraft need to be before vertical takeoff or landing can commence. Too close and perhaps excessive velocities and pressure loading of structures might result; too far away and then aircraft turnaround time is adversely impacted.

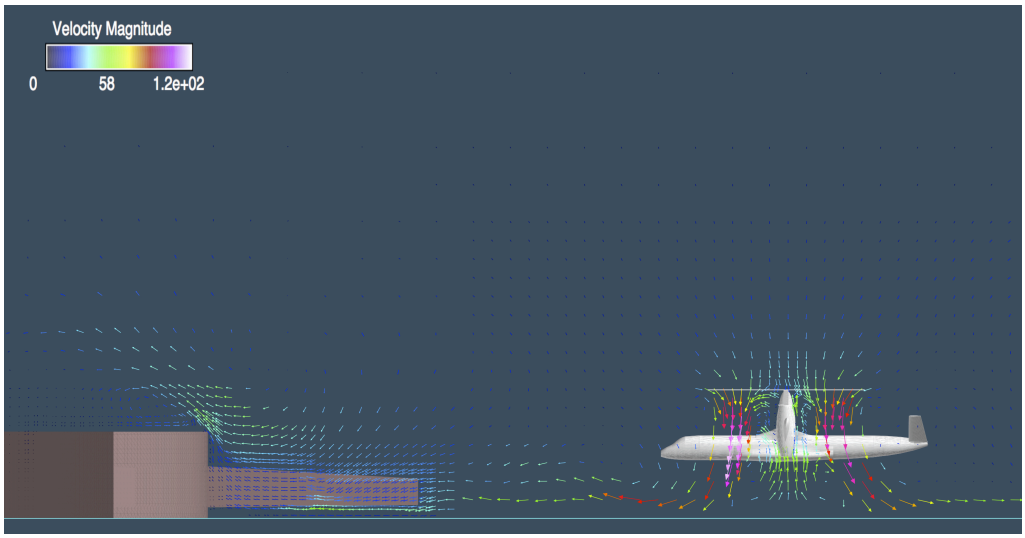

(a) h/R = 1.39

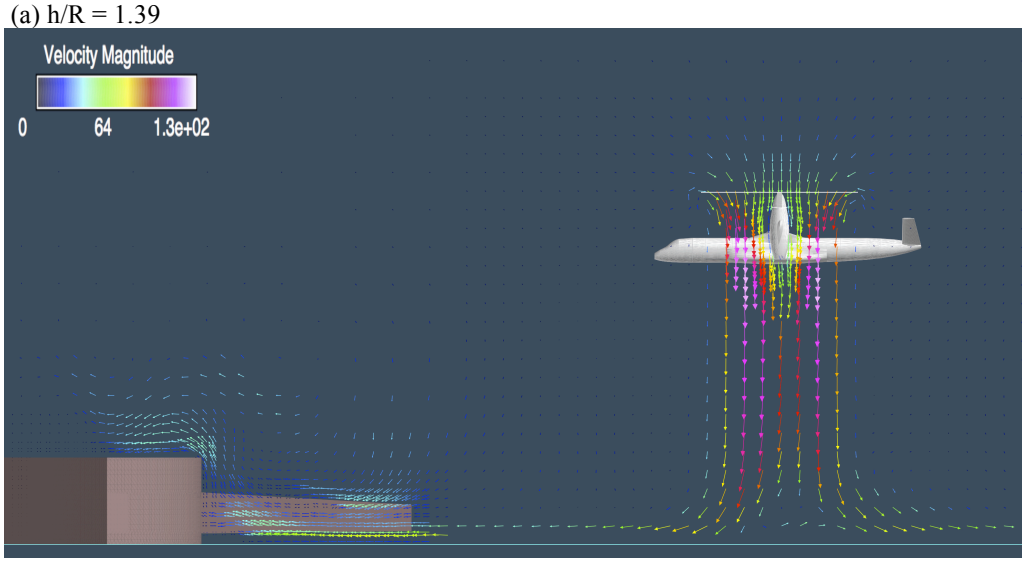

(b) h/R=4.16

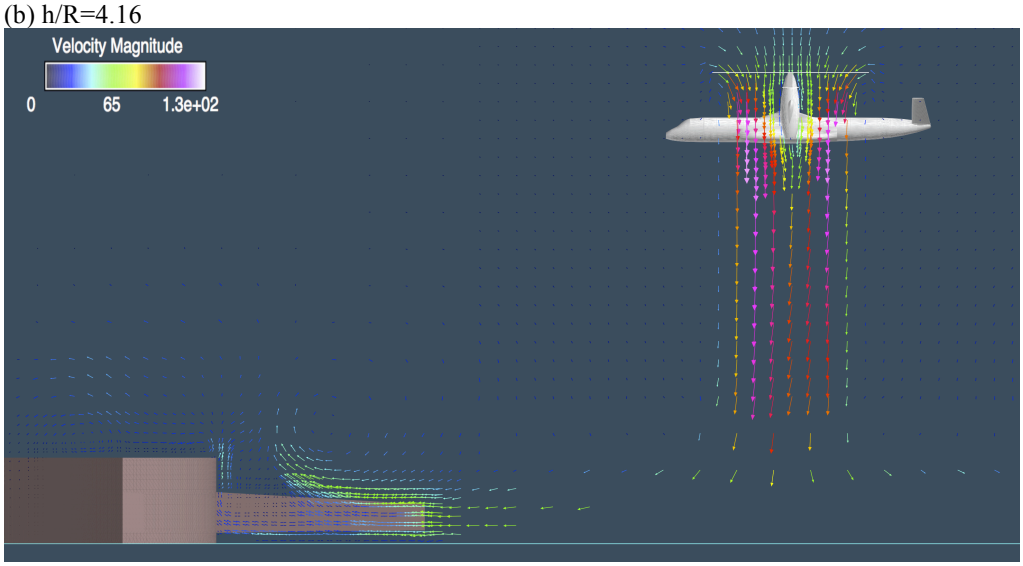

(c) h/R=5.70

Figure 20. LCTR2 operating at varying heights.

Fig. 21 presents some flow field predictions of a LCTR2 overflight over a vertiport terminal building during a simulated takeoff (not necessarily recommended for civil tiltrotor vertiport CONOPS). The interaction of the groundwash with the notional terminal building is significant, particularly for auxiliary structures like the movable jetways for loading and unloading passengers. It is illustrative to contrast Fig. 21 with the Fig. 16 vertical side-plane predictions. The horizontal distance from the LCTR2 to the end of the jetway in Fig. 21 is x/R=4.58, which is the same distance (from the vertical side-plane) as that of Fig. 16b. The jetway is a smaller obstruction to the groundwash than a vertical side-plane and, so, the interaction velocities are more modest in magnitude.

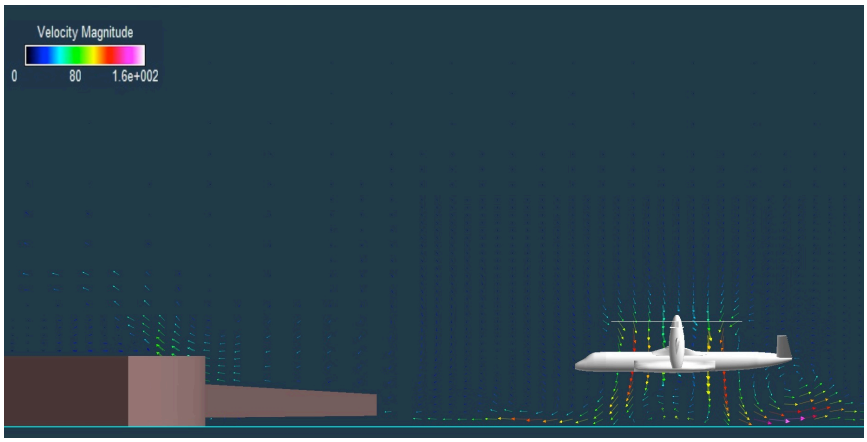

(a) h/R = 1.5 and x/R = 4.58

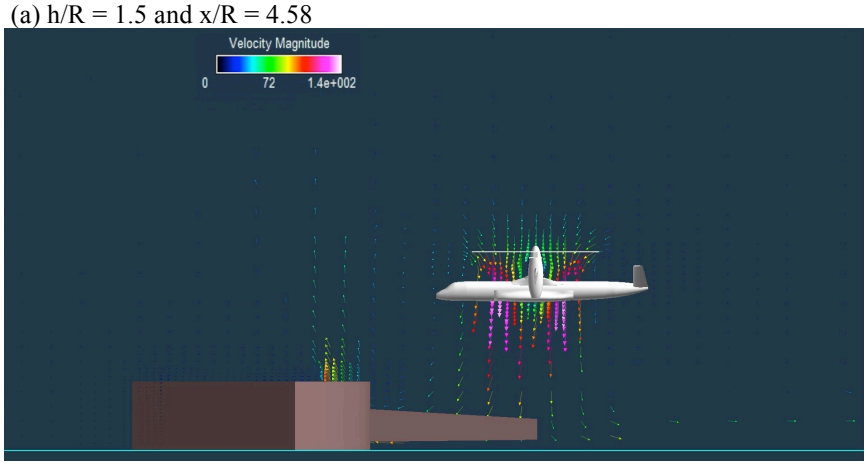

(b) h/R = 3 and x/R = 0

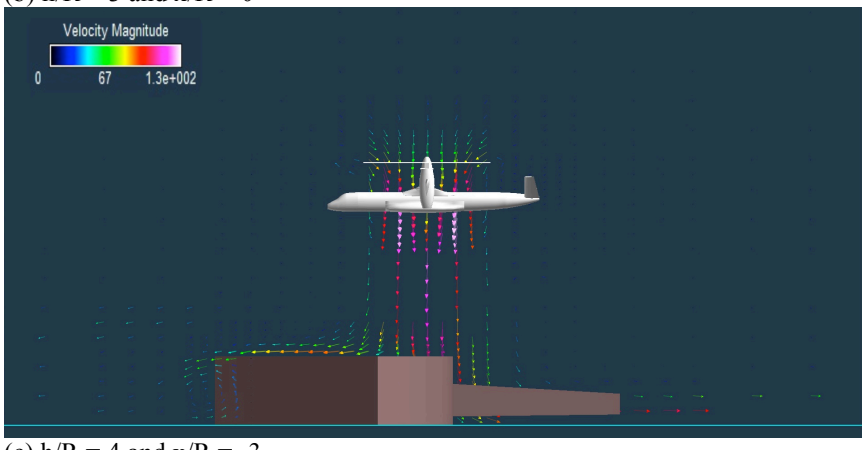

(c) h/R = 4 and x/R = -3

Figure 21. Over-flight of LCTR2 over a notional vertiport building

The consequence of such operations over and near vertiport terminals is the substantial pressure loading of the building structure, shown in Fig. 22. Such pressure loading will undoubtedly be a key consideration in future vertiport terminal building architectural design.

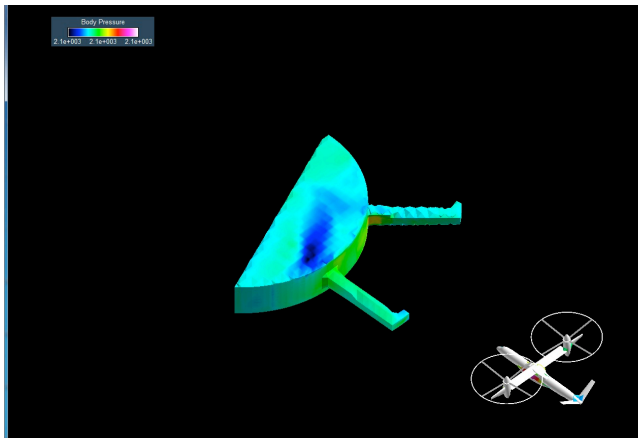

(a) h/R = 1.5 and x/R = 4.58

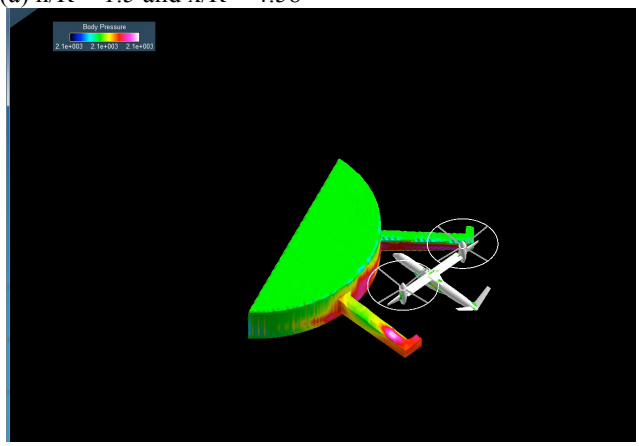

(b) h/R = 3 and x/R = 0

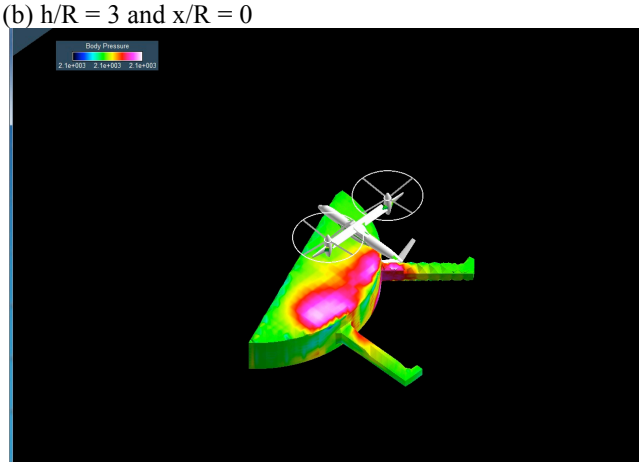

(c) h/R = 4 and x/R = -3

Figure 22. Vertiport building pressure loading due to nearby LCTR2 operation.

D. Interaction with General Aviation Aircraft

An obvious consideration to be explored is tiltrotor wake interactions with surface equipment (tugs, ground vehicles) and small general aviation aircraft. Figure 23 illustrates the type of analysis that will be required to assess operational safety of civil tiltrotors.

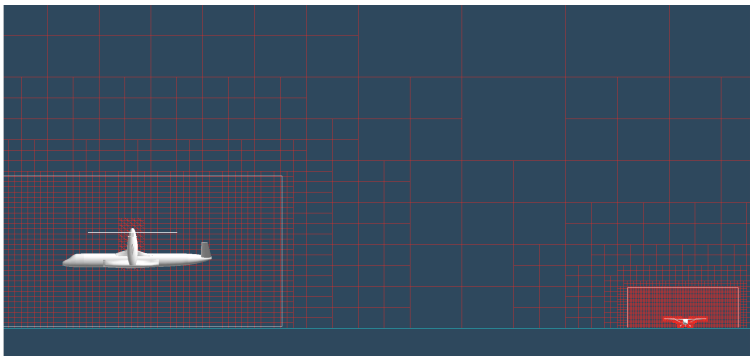

(a) Grid system of LCTR and GA aircraft

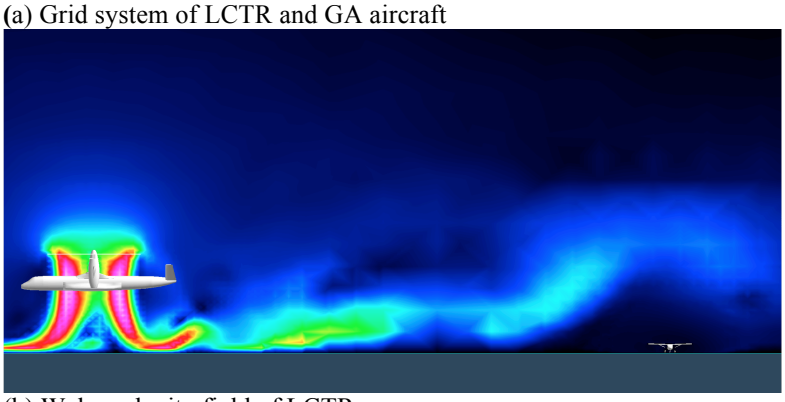

(b) Wake velocity field of LCTR

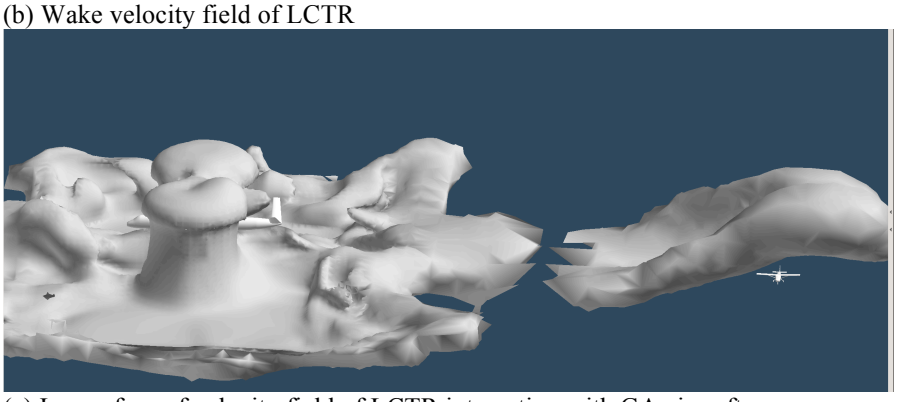

(c) Iso-surface of velocity field of LCTR interacting with GA aircraft.

Figure 23. LCTR2 wake interaction with general aviation aircraft

V. Concluding Remarks

The rotor-induced velocities from large, gross-weight tiltrotors can be potentially hazardous and must be better understood. The outcomes of this study are threefold. First, the information gleaned from this study will help refine future NASA reference designs for civil tiltrotor aircraft. Second, the study can inform future vertiport design considerations. Third, the results can aid the concepts of operation of civil tiltrotors, and rotorcraft in general, in the airport environment such that efficiency and safety are successfully balanced. The results from this study and future similar investigations are necessary to help evaluate operations of this new class of vehicles in the National Airspace System.

RotCFD, a mid-fidelity computational fluid dynamics tool, was successfully used to study the problem of tiltrotor wake interactions (principally groundwash) in the vertiport environment. The analysis is especially tailored for conceptual design studies of rotary-wing vehicles. With a user-friendly interface, complex geometries can be generated with relative ease with this design tool.

Using RotCFD, the NASA civil tiltrotor reference design, LCTR2, was simulated operating in-ground-effect (IGE) near buildings and vertiport structures. The simulations were preceded by simpler isolated rotor(s) studies to validate the analysis.

Specific results from this investigation are as follows:

1. RotCFD predictions compared favorably to well-known rotary-wing aircraft hover and low-speed (edgewise helicopter-mode) forward-flight in-ground-effect analytical models. The general trends with respect to rotor thrust and power with respect to rotor height-above-ground and forward-flight advance ratio were properly captured.
2. An incremental approach was taken to simulate LCTR2 interactions with notional vertiport terminal buildings. Initially predictions were made with respect to large expanse vertical side-planes (simulating vehicle close proximity to large buildings). Then aircraft yaw sweeps were performed with the same large side-planes. Then, finally, a more modestly sized -- and likely more representative -- generic vertiport terminal building was included in the RotCFD study. The predicted downwash/groundwash velocity distributions – and simulated building pressure loading – all appear qualitatively reasonable. Future work will concentrate on performing quantitative validation effort for the RotCFD predictions, using existing experimental data.
3. Finally, a RotCFD modeling demonstration was attempted looking at civil tiltrotor groundwash interactions with a small General Aviation aircraft. Such wake interactions will be an important consideration in future civil tiltrotor operations at airport-based vertiports.

Acknowledgments

This work was supported by the Rotary Wing Project of the Fundamental Aeronautics Program of the NASA Aeronautics Research Mission Directorate and by the NASA SBIR program.

References

[1]Young, L. A., Chung, W. W., Paris, A., Salvano, D., Young, R., Gao, H., Wright, K., and Cheng, V. "Civil Tiltrotor Aircraft Operations," 11th AIAA Aviation Technology, Integration, and Operations (ATIO) Conference, Virginia Beach, VA, Sept. 20-22, 2011.

[2]Young. L.A., Chung, W. W., Paris, A., Salvano, D., Young, R., Gao, H., Wright, K., Miller, D. and Cheng, V. "A Study of Civil Tiltrotor Aircraft in NextGen Airspace," AIAA-2010-9106, 10th AIAA Aviation Technology. Integration, and Operations (ATIO) Conference, Fort Worth, TX, Sept. 13-15, 2010.

[3]Chung, W.W., Linse, D., Paris, A., Salvano, D., Trept, T., Wood, T., Gao, H., Miller, D., Wright, K., Young, R., and Cheng, V., "Modeling High-Speed Civil Tiltrotor Transports in the Next Generation Airspace," NASA CR 2011-215960, October 2011.

[4]Rajagopalan, R. G., Baskaran, V., Hollingsworth, A., Lestari, A., Garrick, D., Solis, E., and Hagerty, B.,"RotCFD - A Tool for Aerodynamic Interference of Rotors: Validation and Capabilities," Future Vertical Lift Aircraft Design Conference, San Francisco, CA, January 18-20, 2012.

[5]Acree, C.W., Yeo H. and Sinsay, J.D., "Performance Optimization of the NASA Large Civil Tiltrotor," Joint AHS/AIAA/SAE/RAeS International Powered Lift Conference (IPLC), London, UK, July 22-24, 2008.

[6]Smith, R. D., Editor, "Heliport/Vertiport Design Deliberations 1997-2000," Report DOT/FAA/ND-00/1, May 2001.

[7]Young, L.A. and Derby, M.R., "Rotor/Wing Interactions in Hover," NASA TM 2002-211392, April 2002.

[8]Rossow, V., "Effect of Ground and Ceiling Planes on Thrust of Rotors in Hover," NASA TM 86754, July 1985.

[9]Johnson, W., *Helicopter Theory*, Princeton University Press, 1980, pp. 122-124.

[10]Patankar, S.V., *Numerical Heat Transfer and Fluid Flow*, Hemisphere Publishing Corp, New York, 1980.

[11]Shih, T. H., Liou, W. W., Shabbir, A., Yang, Z. and Zhiu, J. (1995), " A New Eddy-Viscosity Model for High Reynolds Number Turbulent Flows-Model Development and Validation," Computers and Fluids, 24(3), pp. 227-238.

[12]Johnson, W., "Airloads and Wake Geometry Calculations for an Isolated Tiltrotor Model in a Wind Tunnel," Twenty-Seventh European Rotorcraft Forum, Moscow, Russia, September 11-14, 2001.

[13]FAA Advisory Circular, "Vertiport Design," AC # 150/5390-3, May 31, 1991.

[14]Cheeseman, I.C. and Bennett, W.W., "The Effect of the Ground on a Helicopter Rotor in Forward Flight," ARC RM 3021, 1955. .

[15]Hayden, J.S., "The Effect of the Ground on Helicopter Hovering Power Required," AHS Forum, 1976.